



WANL-PR(Q)-013  
NASA-CR-72316

GPO PRICE \$ \_\_\_\_\_  
CFSTI PRICE(S) \$ \_\_\_\_\_  
Hard copy (HC) \$2.00  
Microfiche (MF) .65

ff 653 July 85

# DEVELOPMENT OF DISPERSION STRENGTHENED TANTALUM BASE ALLOY

Twelfth Quarterly Report

by

R. W. Buckman and R. C. Goodspeed

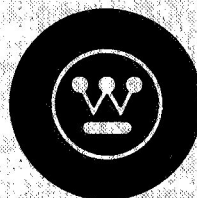
prepared for

National Aeronautics and Space Administration

Lewis Research Center

Space Power Systems Division

Under Contract (NAS 3-2542)



**ASTRONUCLEAR LABORATORY  
WESTINGHOUSE ELECTRIC CORPORATION**

168-13625  
(ACCESSION NUMBER)  
44  
(PAGES)  
CR-72316  
(NASA CR OR TX OR AD NUMBER)

(THRU)  
1  
(CODE)  
17  
(CATEGORY)

FACILITY FORM 602

DEVELOPMENT OF DISPERSION STRENGTHENED  
TANTALUM BASE ALLOY

by

R. W. Buckman, Jr.

and

R. C. Goodspeed

TWELFTH QUARTERLY PROGRESS REPORT

Covering the Period

August 20, 1966 to November 20, 1966

Prepared For

NATIONAL AERONAUTICS AND SPACE ADMINISTRATION  
Contract NAS 3-2542

Technical Management  
Paul E. Moorhead  
NASA-Lewis Research Center  
Space Power Systems Division

Astronuclear Laboratory  
Westinghouse Electric Corporation  
Pittsburgh 36, Pa.

## ABSTRACT

Development of dispersion strengthened tantalum base alloys for use in advanced space power systems continued with the processing of compositions Ta-8W-1Re-1Hf (ASTAR-811) and Ta-7W-1Re-1Hf-0.012C-0.012N (ASTAR-811CN) to 0.04 inch thick sheet. Primary breakdown of the 4 inch diameter consumable electrode melted ingots was by upset or side forging at 1400°C (2550°F) on the Dynapak. Tensile properties were determined over the temperature range of -320 to 3000°F. As-TIG welded sheet specimen of ASTAR-811 and ASTAR-811CN were ductile when bent over a radius of 1t at -320 and -225°F respectively. As-rolled sheet, 33% prior reduction, of both compositions was completely recrystallized after heating for 1 hour at 1600°C. The study of creep properties, phase identification, and effect of heat treatment on phase stability of ASTAR-811 and ASTAR-811CN was initiated. Preliminary results on ASTAR-811CN indicate that only the dimetal carbide is present in the as-cast ingot.

## TABLE OF CONTENTS

	<u>Page No.</u>
I. INTRODUCTION	1
II. PROGRAM STATUS	2
A. FOUR INCH DIAMETER INGOT SCALE-UP	2
III. FUTURE WORK	32
IV. REFERENCES	33



## LIST OF FIGURES

	<u>Page No.</u>
1. Side and Upset Forged Ingots of ASTAR-811	4
2. Side and Upset Forged Ingots of ASTAR-811CN	5
3. Processing Details for ASTAR-811; Heat NASV-22	6
4. Processing Details for ASTAR-811C; Heat NASV-20	7
5. Processing Details for ASTAR-811CN; Heat NASV-23	8
6. Microstructure of 0.04 Inch ASTAR-811 Sheet Annealed 1 Hour at 1650°C (3000°F)	10
7. Microstructure of 0.04 Inch ASTAR-811CN Sheet Annealed 1 Hour at 1650°C (3000°F)	11
8. Average Grain Diameter After 1 Hour Annealing Treatment versus Reciprocal Temperature	14
9. Recrystallization Behavior of ASTAR-811 and ASTAR-811CN	15
10. Yield Strength of ASTAR-811, ASTAR-811C, and ASTAR-811CN	20
11. Fracture Characteristics of ASTAR-811 as a Function of Test Temperature	21
12. Fracture Characteristics of ASTAR-811CN as a Function of Test Temperature	22
13. Unique Microstructures of Two ASTAR-811CN Tensile Specimens	24
14. Creep Properties of ASTAR Tantalum Alloys	26
15. Creep Behavior of T-111	28
16. Creep Behavior of T-111	29
17. Transmission Electron Micrographs of HCP Tantalum Dimetal Carbide	31

## LIST OF TABLES

	<u>Page No.</u>
1. Forging Data for Compositions ASTAR-811, ASTAR-811C, and ASTAR-811CN	3
2. Room Temperature Hardness, Microstructure, and Grain Size of As-Rolled ASTAR-811 Sheet After Annealing for 1 Hour at Temperature	12
3. Room Temperature Hardness, Microstructure, and Grain Size of As-Rolled ASTAR-811CN Sheet After Annealing for 1 Hour at Temperature	13
4. Carbon and Nitrogen Content of ASTAR-811CN as a Function of Heat Treatment Temperature	16
5. Ductile-Brittle Transition Temperature of ASTAR-811, ASTAR-811C, and ASTAR-811CN	18
6. Mechanical Properties of ASTAR-811, ASTAR-811C, and ASTAR-811CN	19
7. Creep Results for ASTAR-811 and ASTAR-811CN at $1 \times 10^{-8}$ Torr	25

## I. INTRODUCTION

This, the twelfth quarterly progress report on the NASA-sponsored program, "Development of Dispersion Strengthened Tantalum Base Alloys" describes the work accomplished during the period August 20 to November 20, 1966. The work was performed under Contract NAS 3-2542.

The primary objective of the current phase of this program is the processing and evaluation of 0.04 inch thick sheet of three compositions which were melted as 60 pound, 4 inch diameter ingots. The compositions were selected for potential sheet and tubing applications on the basis of creep resistance, weldability, and fabricating characteristics.

Prior to this quarterly period, several promising tantalum alloy compositions have been identified which exhibited a good combination of creep resistance, weldability, and fabricability<sup>(1)</sup>. The following three compositions were selected for scale up and were double vacuum, consumable electrode arc melted as 60 pound, 4 inch diameter ingots.

ASTAR-811

Ta-8W-1Re-1Hf

ASTAR-811C

Ta-8W-1Re-1Hf-0.025C

ASTAR-811CN

Ta-8W-1Re-1Hf-0.012C-0.012N

Processing and evaluation of the Ta-8W-1Re-1Hf-0.025C alloy (ASTAR-811C) has been essentially completed<sup>(2)</sup>.

During this quarterly period, ingots of the Ta-8W-1Re-1Hf (ASTAR-811) and Ta-7W-1Re-1Hf-0.012C-0.012N (ASTAR-811CN) alloys were processed to 0.04 inch sheet by a combination of forging and rolling. Evaluation of weldability, fabricability, tensile strength, and creep resistance of the sheet material was initiated.

## II. PROGRAM STATUS

### A. FOUR INCH DIAMETER INGOT SCALE-UP

Primary Working — The remaining portions of the cast ingots of ASTAR-811 (Ta-8W-1Re-1Hf; Heat NASV-22), ASTAR-811C (Ta-8W-1Re-0.7Hf-0.025C; Heat NASV-20), and ASTAR-811CN (Ta-7W-1Re-1Hf-0.012C-0.012N; Heat NASV-23) were sectioned, conditioned, and coated with Al-12Si alloy. Five inch long by four inch diameter sections of ASTAR-811 and ASTAR-811CN were side forged to 1 inch thick plate at 1400°C (2550°F) using three blows of the Dynapak. Four inch diameter x 1-1/4 inch thick as-cast billet sections of all three alloys were heated to 1400°C (2550°F) and then upset forged 40-66% with a single blow of the Dynapak. Forging data are reported in Table 1 and a pictorial view of as-forged billets are shown in Figures 1 and 2. All three compositions exhibited excellent forgeability.

Secondary Working — The ingot sections of NASV-22 and NASV-23, upset forged during the previous report period<sup>(2)</sup>, were conditioned, annealed for 1 hour at 1650°C (3000°F), and rolled to 0.06 inch sheet. This sheet was then conditioned, annealed for 1 hour at 1700°C (3270°F), and rolled to 0.04 inch sheet. Specimens for the evaluation of weldability, mechanical properties, and creep resistance described in this report were taken from this material. The remaining upset forged billets were conditioned and are being processed to sheet.

The side forged billets of NASV-22 and NASV-23 (ASTAR-811 and ASTAR-811CN) were conditioned, annealed for 1 hour to 1480°C (2700°F), and rolled to approximately 0.33 inch plate at 260°C (500°F). Several sections cut from each plate were then annealed for 1 hour at 1650°C (3000°F) and combination straight and cross rolled at room temperature to 0.04 inch sheet measuring 4 to 5 inches wide and 14 to 28 inches long. The fabricability of both of these alloys is excellent.

The complete processing schedules for NASV-22 (ASTAR-811), NASV-20, (ASTAR-811C), and NASV-23 (ASTAR-811CN) are shown in Figures 3, 4, and 5 respectively. Also included are the dimensions, weights, and hardnesses at the various stages of processing.

TABLE 1 - Forging Data for Compositions ASTAR-811 (Ta-8W-1Re-1Hf), ASTAR-811C (Ta-8W-1Re-0.7Hf-0.025C) and ASTAR-811CN (Ta-7W-1Re-1Hf-0.012C-0.012N)

Composition and Heat Number	Type of Forging	Forging Temperature (°C) (°F)	Weight (lbs.)	Initial Size (inches)	Final Size (inches)	Reduction (%)	Constant (K <sub>u</sub> ) <sup>(a)</sup> (psi)
ASTAR-811C Ta-8W-1Re-0.7Hf-0.025C (Heat NASV-20)	Upset	1400 2550	9.75	1-3/8t x 3.85D	0.821t x 4-7/8D	40	146,000
	Upset	1400 2550	9.37	1-3/8t x 3.85D	0.566t x 5-3/4D	59	130,000
	Side <sup>(b)</sup>	1400 2550	35.37	5t x 3.85D	1.174t x 7-1/2 x 7-3/4	66 <sup>(c)</sup>	99,000 <sup>(c)</sup>
ASTAR-811 Ta-8W-1Re-1Hf (Heat NASV-22)	Upset	1400 2550	7.56	1-1/8t x 3.85D	0.385t x 6-3/8D	66	108,000
	Upset	1400 2550	8.00	1-1/8t x 3.85D	0.418t x 6-1/4D	63	116,000
	Side <sup>(b)</sup>	1400 2550	36.00	5t x 3.85D	1.276t x 7 x 7-1/4	63 <sup>(c)</sup>	146,000 <sup>(c)</sup>
ASTAR-811CN Ta-7W-1Re-1Hf-0.012C-0.012N (Heat NASV-23)	Upset	1400 2550	10.19	1-3/8t x 3.85D	0.670t x 5-1/2D	51	147,000

(a)  $K_u = \frac{E}{VZ}$  where E = energy used, V = volume of material deformed, and Z = empirical upset factor.

(b) Three blows on Dynapak.

(c) Corrected for geometry.

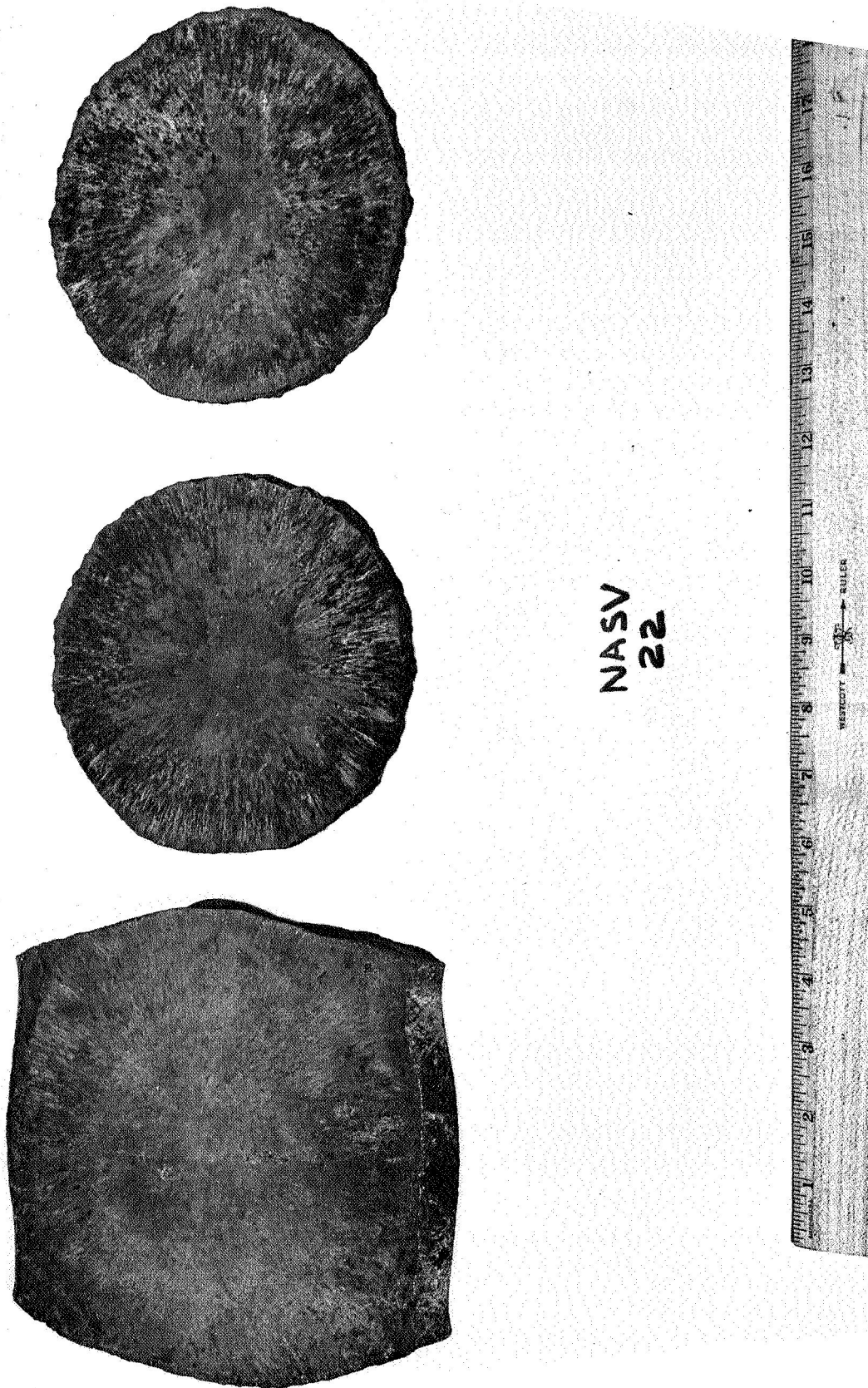


FIGURE 1 – Side and Upset Forged Ingots of ASTAR-811

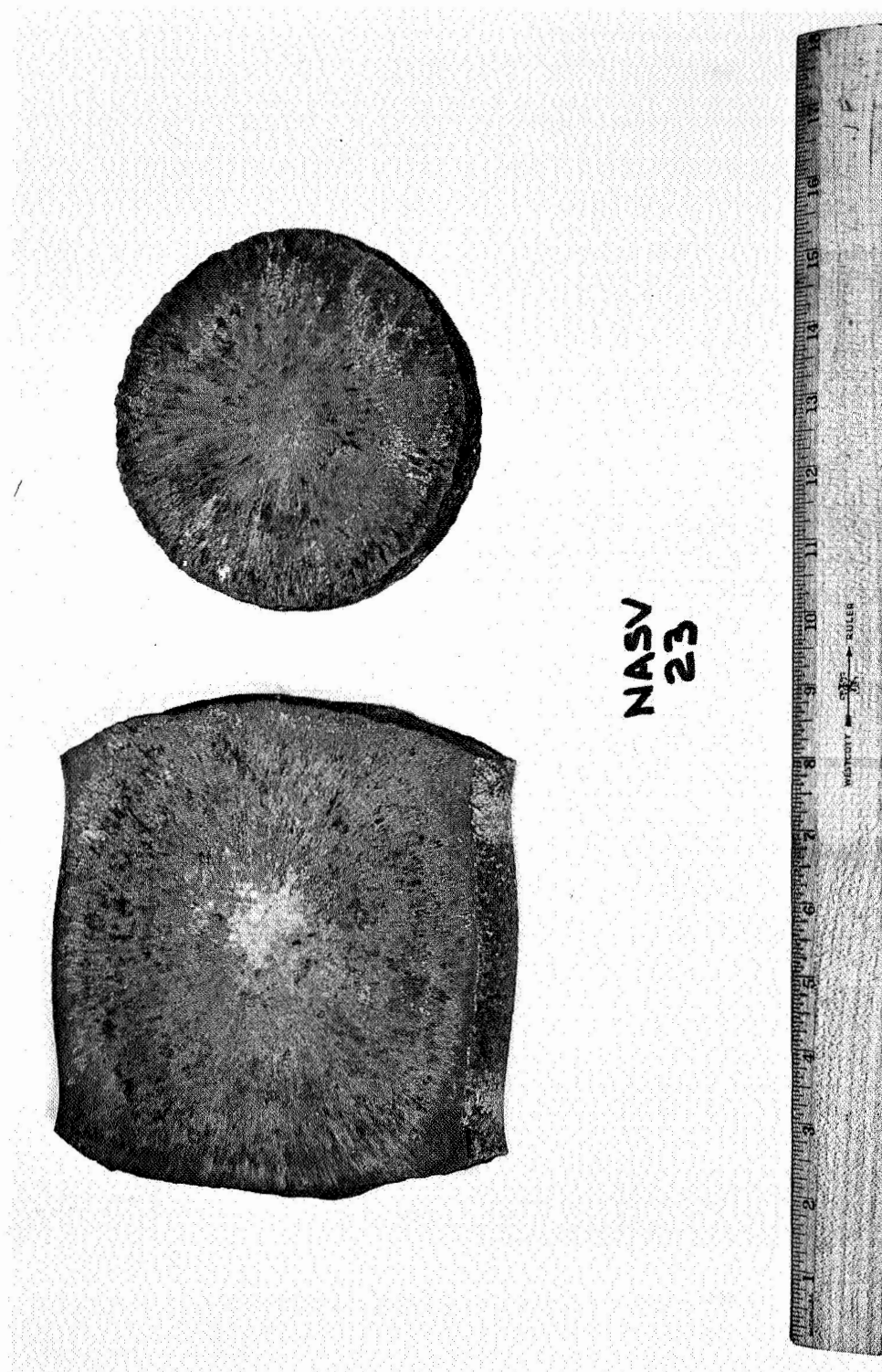


FIGURE 2 - Side and Upset Forged Ingots of ASTAR-811CN

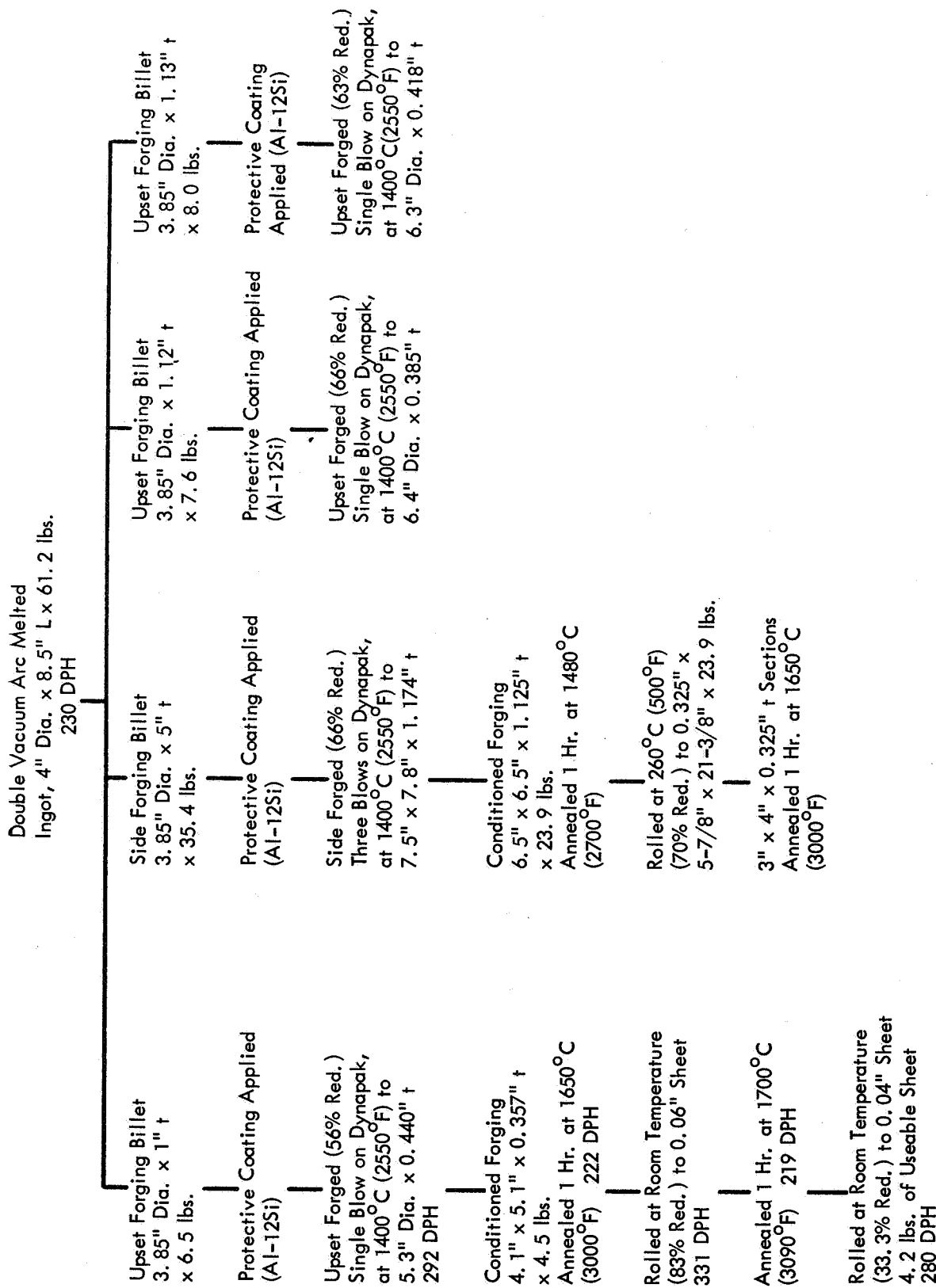
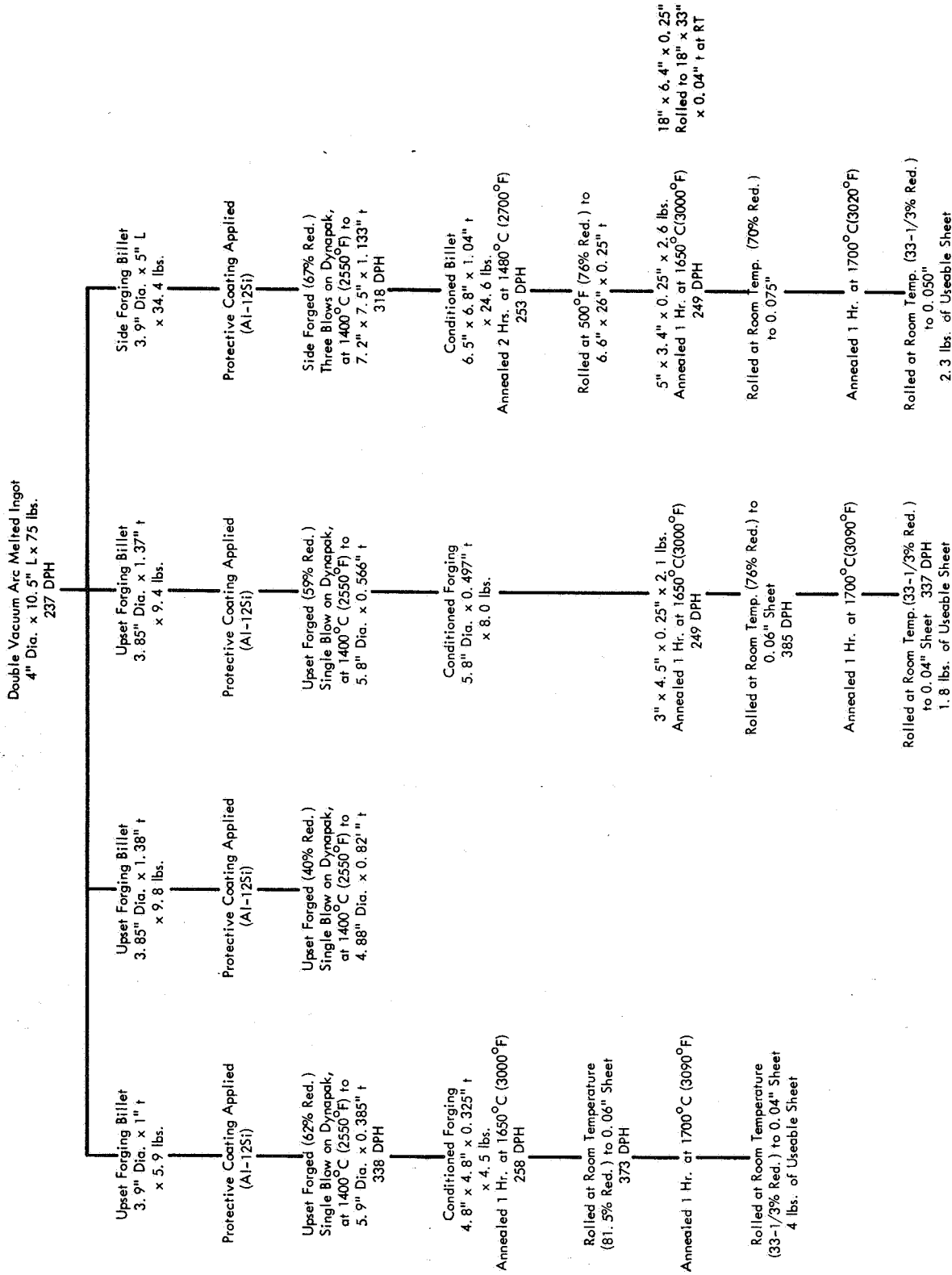


FIGURE 3 - Processing Details for ASTAR-811; Heat NASV-22





**FIGURE 4 – Processing Details for ASTAR-811C; Heat NASV-20**

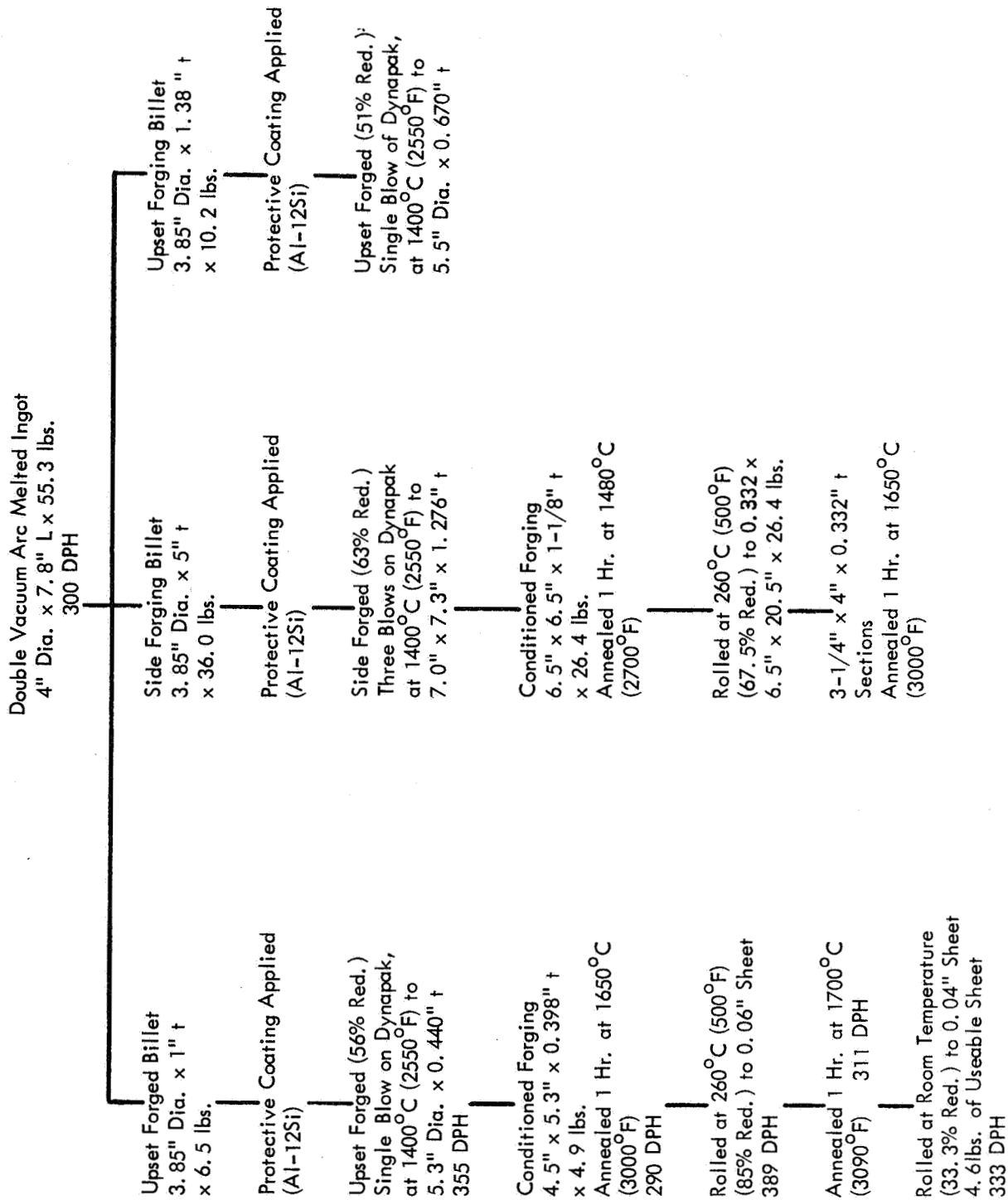


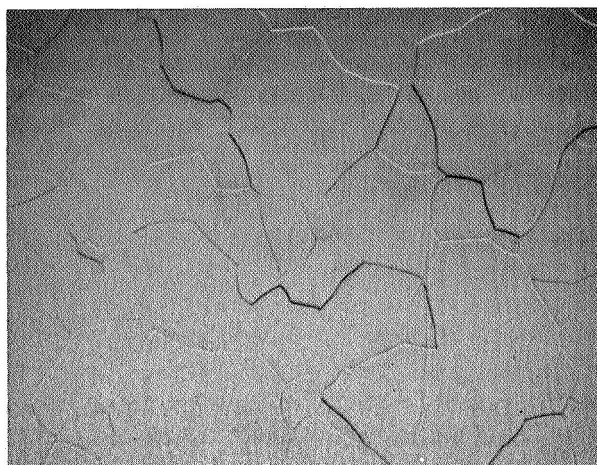
FIGURE 5 - Processing Details for ASTAR-811CN; Heat NASV-23

The microstructures of 0.04 inch ASTAR-811 and ASTAR-811CN sheet annealed for 1 hour at 1650°C are shown in Figures 6 and 7 respectively. The precipitate visible in the ASTAR-811CN matrix is presumed to be the tantalum dimetal carbide.

Recrystallization Behavior — The effect of 1 hour annealing treatments on the microstructure, hardness, and grain size of ASTAR-811 (Heat NASV-22) and ASTAR-811CN (NASV-23) was investigated. As-rolled 0.06 inch and 0.04 inch thick sheet which had been reduced 85 and 33% respectively was heated for 1 hour at temperatures ranging from 1200 to 2200°C (2190 to 3990°F). The resulting microstructural grain size and hardness data are tabulated in Tables 2 and 3 and plotted in Figures 8 and 9. The difference in recrystallization behavior between ASTAR-811 and ASTAR-811CN is slight. As expected, the higher the amount of prior deformation, the finer the recrystallized grain size. However, at temperatures above 1800–1900°C, rapid grain growth predominates and the effect of the prior deformation is negligible.

The shape of the isochronal annealing curve for ASTAR-811 is normal for a low interstitial containing tantalum alloy matrix with minimum hardness occurring prior to formation of an equiaxed microstructure. ASTAR-811CN exhibited a typical isochronal annealing curve with a hardness minima occurring at approximately 1400°C. However the continuing decrease in hardness for specimens heated above 1800°C was attributed to the possible loss of carbon and nitrogen during annealing. That both carbon and nitrogen were lost during the 1 hour heat treatments was verified by chemical analysis. These data are reported in Table 4. It has been standard practice to wrap all specimens for heat treatment in pure tantalum foils which acts as an additional barrier to contamination during heating at  $10^{-5}$  to  $10^{-6}$  torr. Previous work has shown that the tantalum foil acts as a sink for carbon<sup>(1)</sup>. High temperature vacuum annealing studies are being repeated on both wrapped and bare specimens to evaluate the degree of carbon and nitrogen loss during high temperature vacuum annealing treatments.

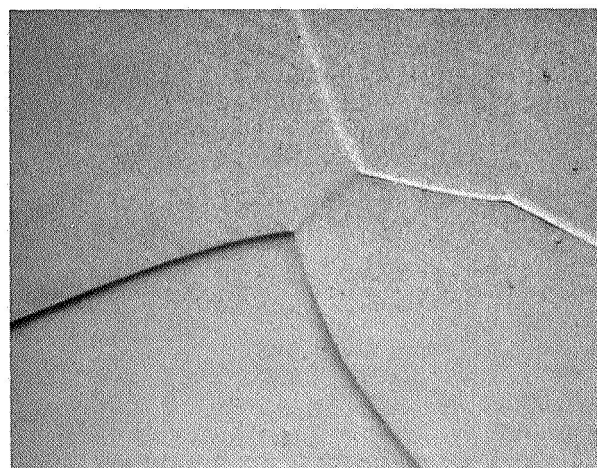
Weldability — Electron beam (EB) and tungsten inert gas (TIG) bead-on-plate welds were made on 0.04 inch ASTAR-811 (NASV-22) and ASTAR-811CN (NASV-23) sheet, which had been annealed for 1 hour at 1650°C (3000°F) prior to welding. Ductile-brittle transition



(a) 150X

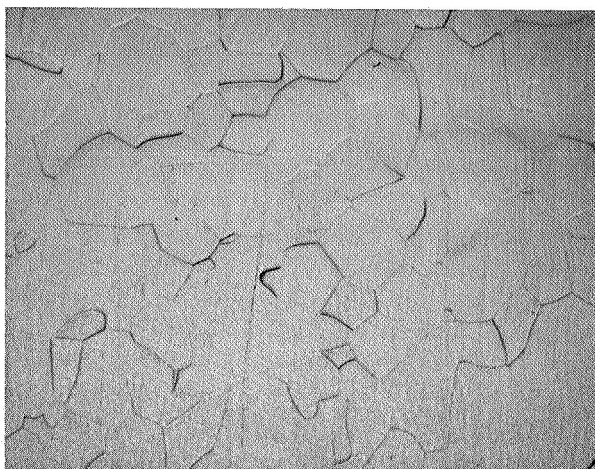


(b) 500X

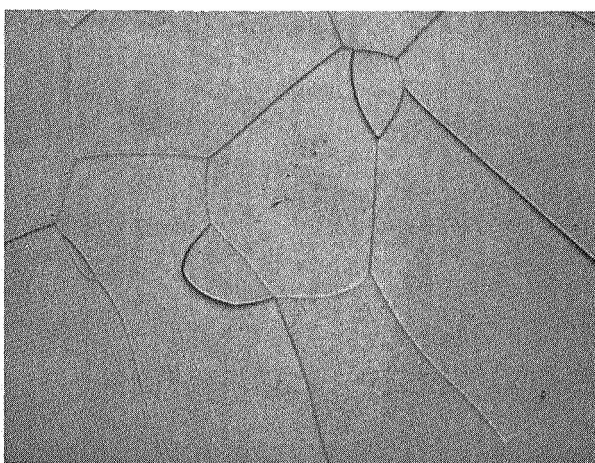


(c) 1500X

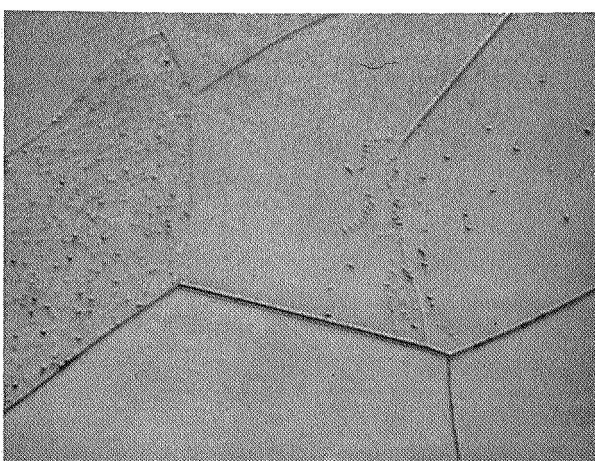
**FIGURE 6 - Microstructure of 0.04 Inch ASTAR-811 (Ta-8W-1Re-1Hf) Sheet  
Annealed 1 Hour at 1650°C (3000°F) Oblique Light.**



(a) 150X



(b) 500X



(c) 1500X

**FIGURE 7 - Microstructure of 0.04 Inch ASTAR-811CN (Ta-7W-1Re-1Hf-0.012C-0.012N) Sheet Annealed One Hour at 1650°C (3000°F) Oblique Light**

TABLE 2 - Room Temperature Hardness<sup>(a)</sup>, Microstructure<sup>(b)</sup>, and Grain Size<sup>(c)</sup> of As-Rolled  
ASTAR-811(Heat NASV-22) Sheet After Annealing for One Hour at Temperature

Sheet Thickness	Prior Reduction (%)	As-Rolled	One Hour Annealing Temperature (°C/°F)										
			1200 2190	1300 2370	1400 2550	1500 2730	1600 2910	1700 3090	1800 3270	1900 3450	2000 3630	2100 3810	2200 3990
0.04" Sheet Hardness Microstructure Grain Size	33.3	280 W	225 W	232 W	228 R <sub>5</sub>	216 R <sub>85</sub>	206 R <sub>x</sub>	200 R <sub>x</sub>	201 R <sub>x</sub>	200 R <sub>x</sub>	198 R <sub>x</sub>	201 R <sub>x</sub>	209 R <sub>x</sub>
						0.047	0.048	0.091	0.108	0.148	0.240	0.500	
0.06" Sheet Hardness Microstructure Grain Size	83.0	331 W	308 W	260 R <sub>5</sub>	218 R <sub>90</sub>	217 R <sub>x</sub>	217 R <sub>x</sub>	219 R <sub>x</sub>	215 R <sub>x</sub>	216 R <sub>x</sub>	213 R <sub>x</sub>	219 R <sub>x</sub>	221 R <sub>x</sub>
						0.016	0.020	0.039	0.052	0.080	0.129	0.240	0.615

(a) DPH, 30 Kg Load

(b) Microstructure: W = Wrought

R<sub>5</sub> = About 5% Recrystallized

R<sub>85</sub> = About 85% Recrystallized

R<sub>90</sub> = About 90% Recrystallized

R<sub>x</sub> = Fully Recrystallized

(c) Grain size in mm, as determined by standard line intercept method.

TABLE 3 - Room Temperature Hardness<sup>(a)</sup>, Microstructure<sup>(b)</sup>, and Grain Size<sup>(c)</sup> of As-Rolled  
ASTAR-811CN(Heat NASV-23) Sheet After Annealing for One Hour at Temperature

Sheet Thickness	Prior Reduction (%)	As-Rolled	One Hour Annealing Temperature (°C/°F)										
			1200 2190	1300 2370	1400 2550	1500 2730	1600 2910	1700 3090	1800 3270	1900 3450	2000 3630	2100 3810	2200 3990
0.04" Sheet	33.3	333 W	319 W	301 W	288 W	281 R <sub>35</sub>	293 R <sub>x</sub>	298 R <sub>x</sub>	296 R <sub>x</sub>	282 R <sub>x</sub>	276 R <sub>x</sub>	236 R <sub>x</sub>	223 R <sub>x</sub>
						0.033	0.047	0.058	0.115	0.175	0.235	0.325	
0.06" Sheet	85.0	389 W	355 W	336 W	302 R <sub>5</sub>	304 R <sub>95</sub>	312 R <sub>x</sub>	311 R <sub>x</sub>	318 R <sub>x</sub>	294 R <sub>x</sub>	282 R <sub>x</sub>	258 R <sub>x</sub>	240 R <sub>x</sub>
						0.016	0.035	0.048	0.095	0.170	0.220	0.380	

(a) DPH, 30 Kg Load

(b) Microstructure: W = Wrought

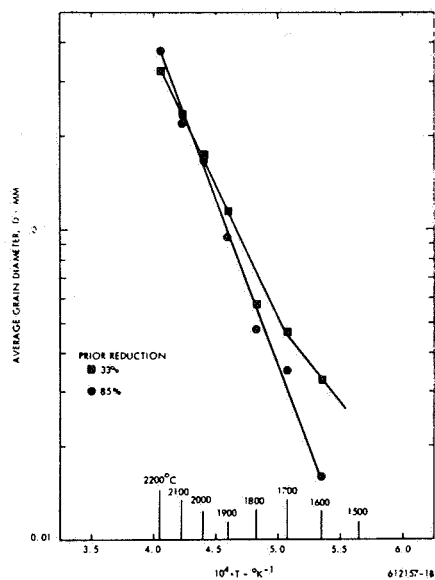
R<sub>5</sub> = About 5% Recrystallized

R<sub>35</sub> = About 35% Recrystallized

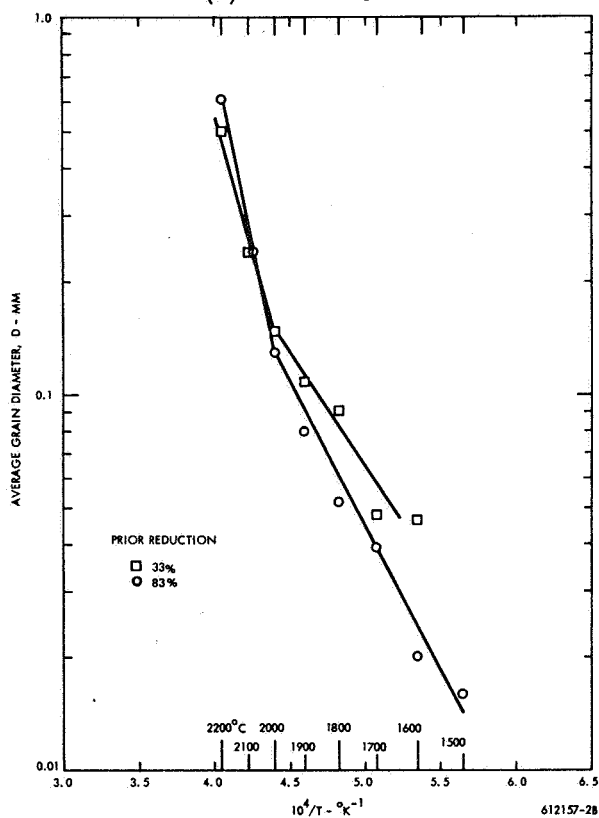
R<sub>95</sub> = About 95% Recrystallized

R<sub>x</sub> = Fully Recrystallized

(c) Grain size in mm, as determined by standard line intercept method.



(a) ASTAR-811CN



(b) ASTAR-811

FIGURE 8 - Average Grain Diameter After 1 Hour Annealing Treatment versus Reciprocal Temperature



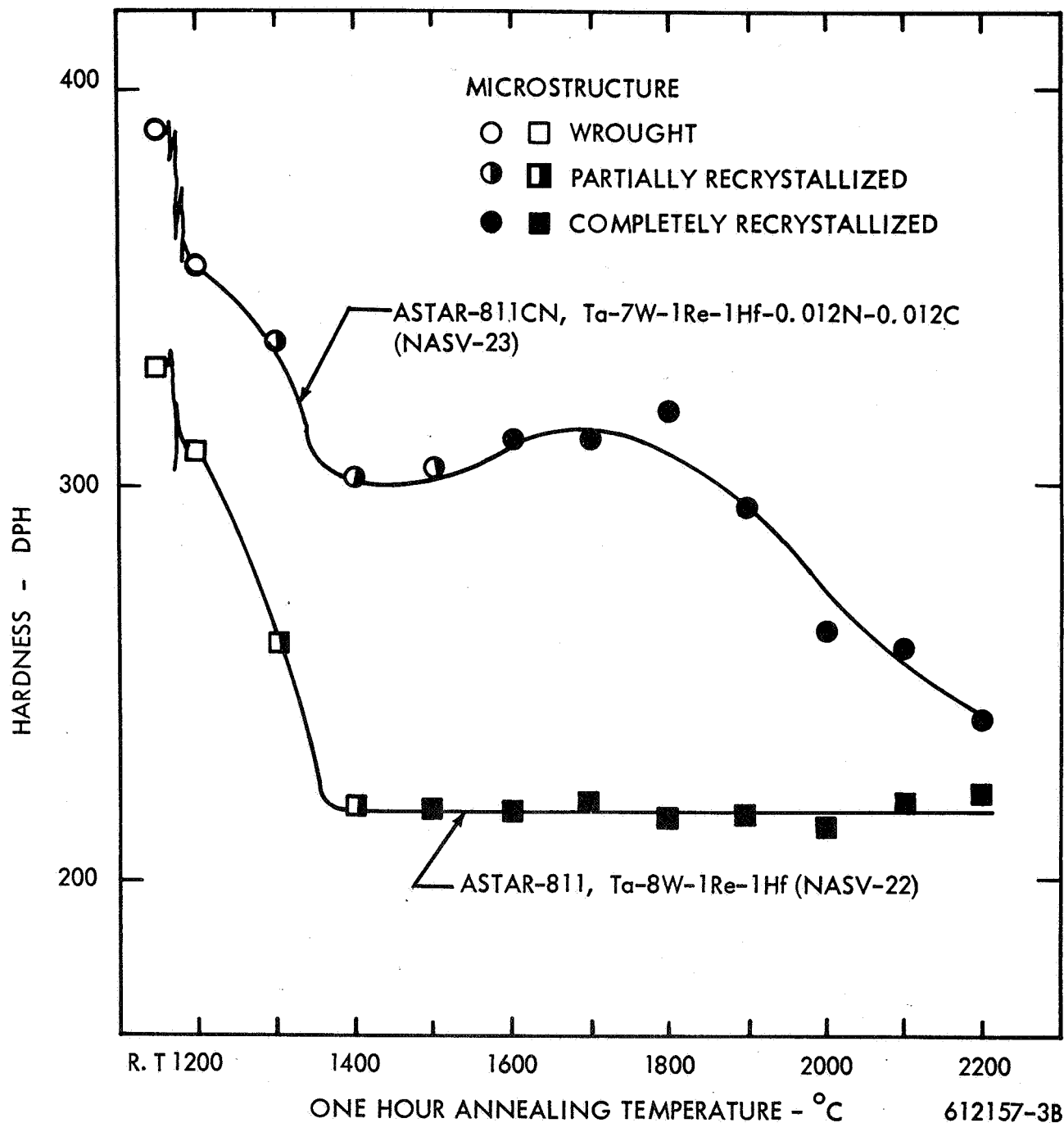


FIGURE 9 - Recrystallization Behavior of ASTAR-811 and ASTAR-811CN

**TABLE 4 - Carbon and Nitrogen Content of ASTAR-811CN  
as a Function of Heat Treatment<sup>(a)</sup> Temperature**

Temperature °C/°F	Carbon Analyses(ppm)	
	Carbon	Nitrogen
1650/3000	123 <sup>(b)</sup>	125 <sup>(b)</sup>
2000/3630	89	87
2100/3810	25	78
2200/3990	10	72

(a) One hour heat treatments with 0.04 inch thick sheet specimens wrapped in Ta foil.

(b) Average of three analyses.

temperatures of the welded and of base metal samples were determined. The results, along with those previously obtained on ASTAR-811C (NASV-20) sheet, are summarized in Table 5. The transition temperature of both ASTAR-811 and ASTAR-811CN in all three of the tested conditions was less than  $-320^{\circ}\text{F}$  ( $-195^{\circ}\text{C}$ ), with the exception of a transition temperature of  $-225^{\circ}\text{F}$  ( $-143^{\circ}\text{C}$ ) for ASTAR-811CN in the as-TIG welded condition. The intrinsic ductility for all three compositions is excellent as evidenced by the ductile-brittle behavior of TIG welded material.

### Mechanical Property Evaluation

a. Tensile Data — Tensile data were obtained on 0.04 inch thick sheet specimens of ASTAR-811 (NASV-22) and ASTAR-811CN (NASV-23) at  $-320$ ,  $-150$ ,  $70$ ,  $600$ ,  $2200$ ,  $2400$ ,  $2600$ , and  $3000^{\circ}\text{F}$  ( $-195$ ,  $-101$ ,  $21$ ,  $315$ ,  $1205$ ,  $1315$ ,  $1427$ , and  $1650^{\circ}\text{C}$ ). The sheet was processed from upset forgings and the specimens were annealed for 1 hour at  $1650^{\circ}\text{C}$  ( $3000^{\circ}\text{F}$ ) prior to testing. The tensile data are recorded in Table 6, and the yield strengths are plotted in Figure 10. Also included are the previously obtained data on ASTAR-811C. Both carbon and nitrogen additions raise the short time tensile properties of the Ta-W-Re-Hf matrix over the range of  $-320^{\circ}\text{F}$  to  $2600^{\circ}\text{F}$ . Above  $2600^{\circ}\text{F}$ , C and/or N additions at these concentration levels make no contribution to the tensile strength. The potent effectiveness of nitrogen on tensile properties is apparent. Tensile ductility for all three compositions was similar with the exception of the ASTAR-811 which exhibited only 10% elongation at  $3000^{\circ}\text{F}$  compared to 32% for the ASTAR-811CN.

Fracture characteristics of these tensile specimens were metallographically studied. The results are shown in Figures 11 and 12 for ASTAR-811 and ASTAR-811CN specimens respectively. At low temperatures, failure of ASTAR-811 occurred predominantly by shear, even at  $-320^{\circ}\text{F}$  ( $-195^{\circ}\text{C}$ ), while the ASTAR-811CN specimens exhibited considerable intergranular fracture, similar to that exhibited by ASTAR-811C. At the elevated temperatures, extensive intergranular fracture was observed in both the ASTAR-811 and ASTAR-811CN specimens. In fact at  $2400^{\circ}\text{F}$  ( $1315^{\circ}\text{C}$ ), ASTAR-811C exhibited considerably more shear failure than did either of the other alloys which may be indicative of boundary strengthening by the carbide phase.

TABLE 5 - Ductile-Brittle Transition Temperature<sup>(a)</sup> of ASTAR-811, ASTAR-811C, and ASTAR-811CN

Composition and Heat Number	Condition	Temperature (°F) (°C)		No Load Bend Angle(Degrees)	Remarks	DBTT (°F) (°C)	
ASTAR-811 <sup>(b)</sup> Ta-8W-1Re-1Hf (Heat NASV-22)	Base Metal Electron Beam Welded TIG Welded	-320	-195	92	Bend	<-320	<-195
		-320	-195	90	Bend	<-320	<-195
		-320	-195	91	Bend	<-320	<-195
ASTAR-811C <sup>(c)</sup> Ta-8W-1Re-0.7Hf-0.025C (Heat NASV-20)	Base Metal Electron Beam Welded TIG Welded	-320	-195	96	Bend	<-320	<-195
		-320	-195	96	Bend	<-320	<-195
						-175 to -250	-115 to -157
ASTAR-811CN <sup>(b)</sup> Ta-7W-1Re-1Hf-0.012C-0.012N (Heat NASV-23)	Base Metal Electron Beam Welded TIG Welded	-320	-195	89	Bend	<-320	<-195
		-320	-195	89	Bend	<-320	<-195
		-250	-157	90	Failure		
		-225	-143	91	Bend	-225	-143

(a) Sheet materials annealed for 1 hour at 1650°C(3000°F) prior to welding and/or testing.

(b) 0.040 inch sheet and 1.0t bend radius used.

(c) 0.040 inch sheet and 1.8t bend radius used.

TABLE 6 - Mechanical Properties<sup>(a)</sup> of ASTAR-811, ASTAR-811C, and ASTAR-811CN

Composition and Heat Number	Test Temperature (°F)	0.2% Yield Strength <sup>(b)</sup> (ksi)	Ultimate Tensile Strength <sup>(b)</sup> (ksi)	Elongation		Reduction in Area (%)
				Uniform (%)	Total (%)	
ASTAR-811 Ta-8W-1Re-1Hf (Heat NASV-22)	-320	134.5	147.8	24.6	31.4	62.6
	-150	97.6	113.2	18.9	29.4	61.6
	-RT	76.0	88.0	19.3	33.4	66.2
	+600	42.2	55.0	18.1	28.1	51.3
	2200	38.7	40.4	----	30.3	----
	2400	22.6	33.7	----	28.9	----
	2600	21.8	28.7	----	28.6	----
ASTAR-811C Ta-8W-1Re-0.7Hf-0.025C (Heat NASV-20)	3000	22.1	22.9	----	10.9	----
	-320	147.7	165.3	22.1	26.3	42.0
	-150	111.0	130.3	20.1	28.5	46.3
	RT	85.0	105.4	17.0	25.9	50.0
	RT	85.3	103.5	15.5	26.6	48.4
	RT	82.8	104.6	16.4	27.6	49.3
	+600	53.7	75.5	15.3	24.5	47.9
	1500	41.3	79.6	----	18.8	----
	2000	35.0	60.9	----	24.0	----
	2200	31.6	49.9	----	28.8	----
ASTAR-811CN Ta-7W-1Re-1Hf-0.012C-0.012N (Heat NASV-23)	2400	30.4	40.9	----	35.0	----
	2600	29.5	35.3	----	34.8	----
	2800	23.0	28.4	----	49.5	----
	-320	177.5	189.0	14.2	21.6	38.2
	-150	140.0	145.8	12.6	23.7	53.0
	RT	110.3	117.3	14.4	25.4	56.0
	+600	63.0	77.5	15.9	23.8	53.1
	2200	35.8	57.3	----	17.7	----
	2400	31.5	45.5	----	24.6	----
	2600	26.8	36.0	----	20.1	----
	3000	20.9	21.5	----	31.6	----

(a) Specimens annealed for 1 hour at 1650°C(3000°F) prior to test.

(b) Strain rate of 0.05 in/min throughout test.

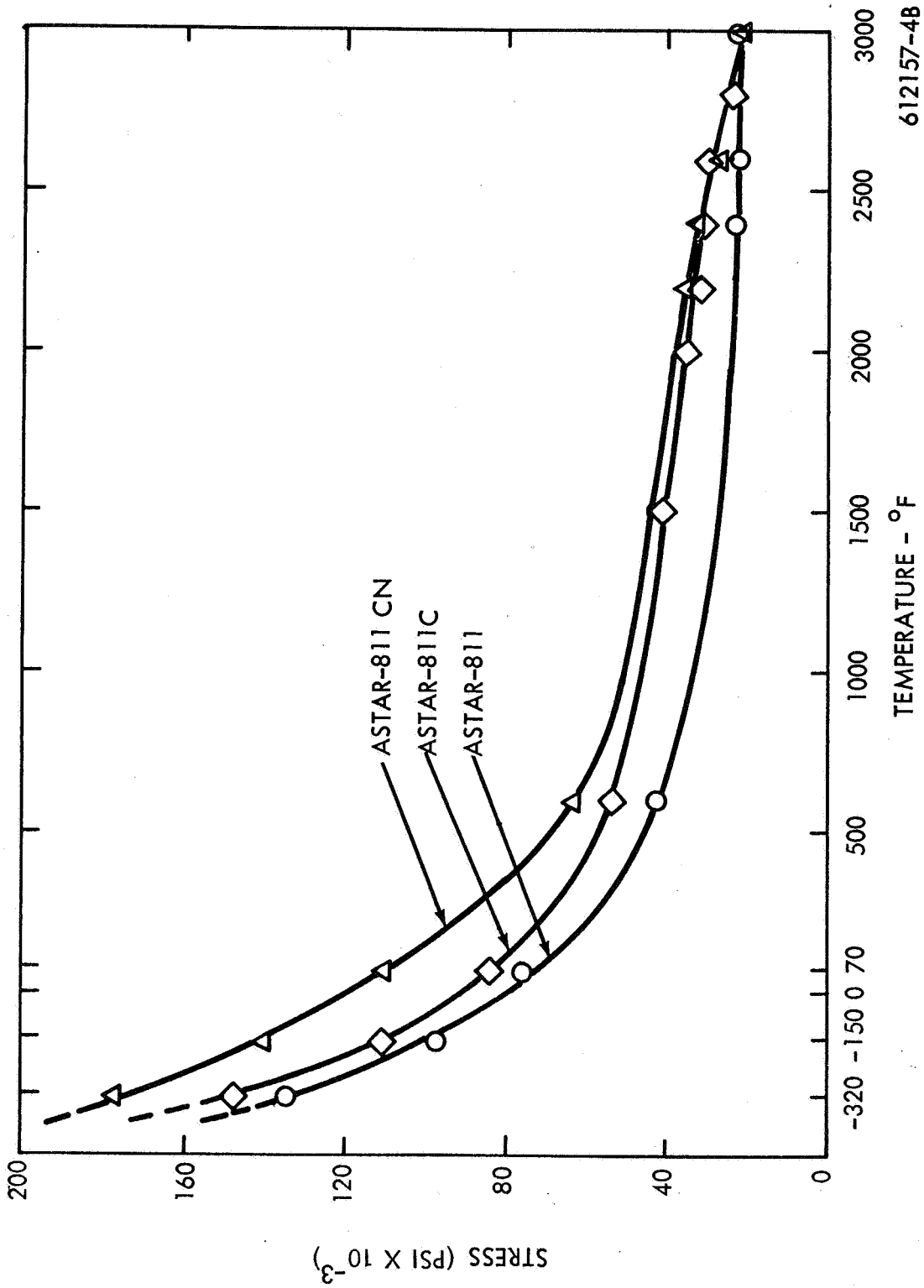


FIGURE 10 - Yield Strengths of ASTAR-811 (Ta-8W-1Re-1Hf), ASTAR-811C (Ta-8W-1Re-0.7Hf-0.025C), and ASTAR-811CN (Ta-7W-1Re-1Hf-0.012C-0.012N) 612157-4B

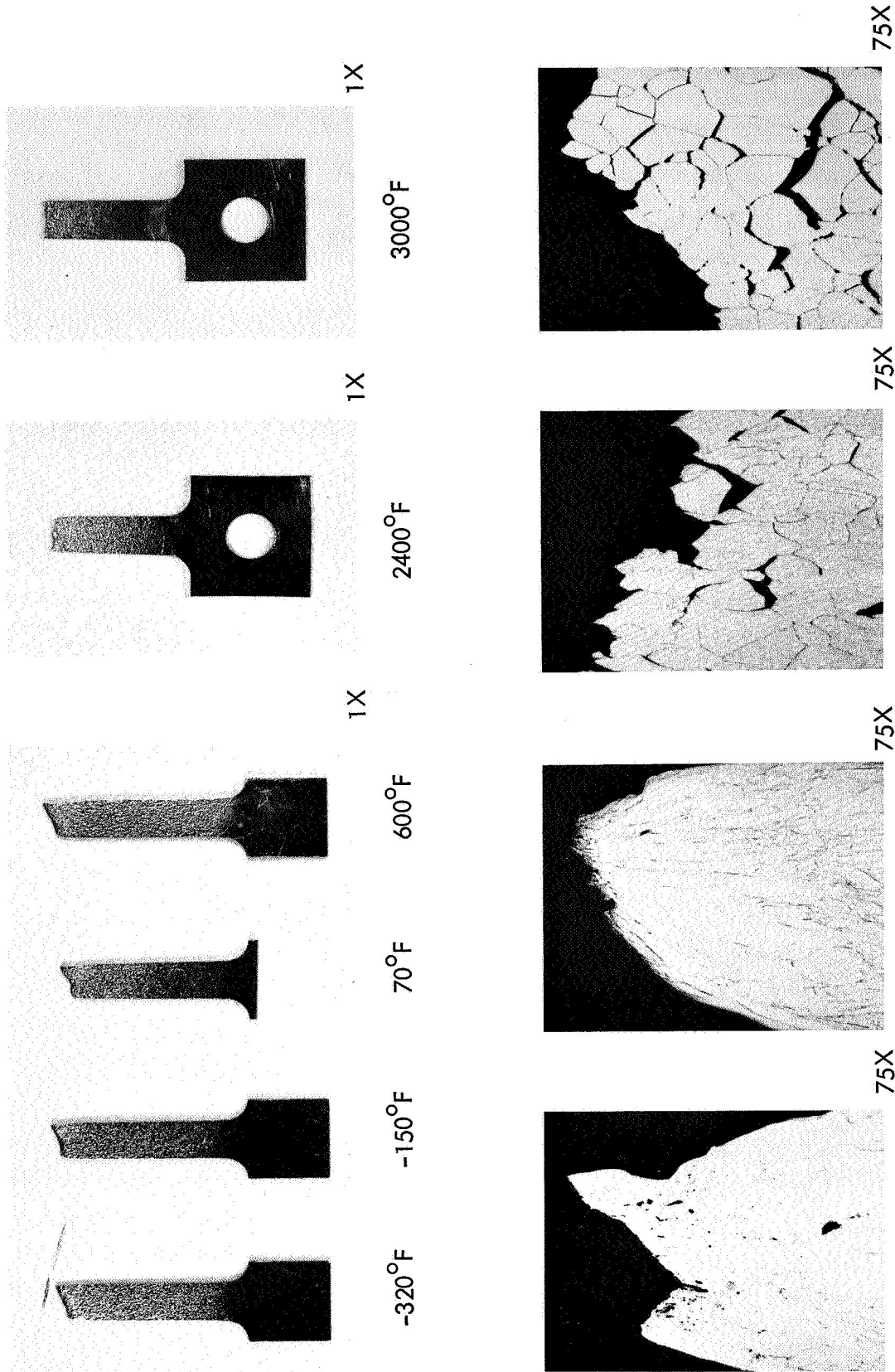


FIGURE 11 - Fracture Characteristics of ASTAR-811 (Ta-8W-1Re-1Hf) as a Function of Test Temperature

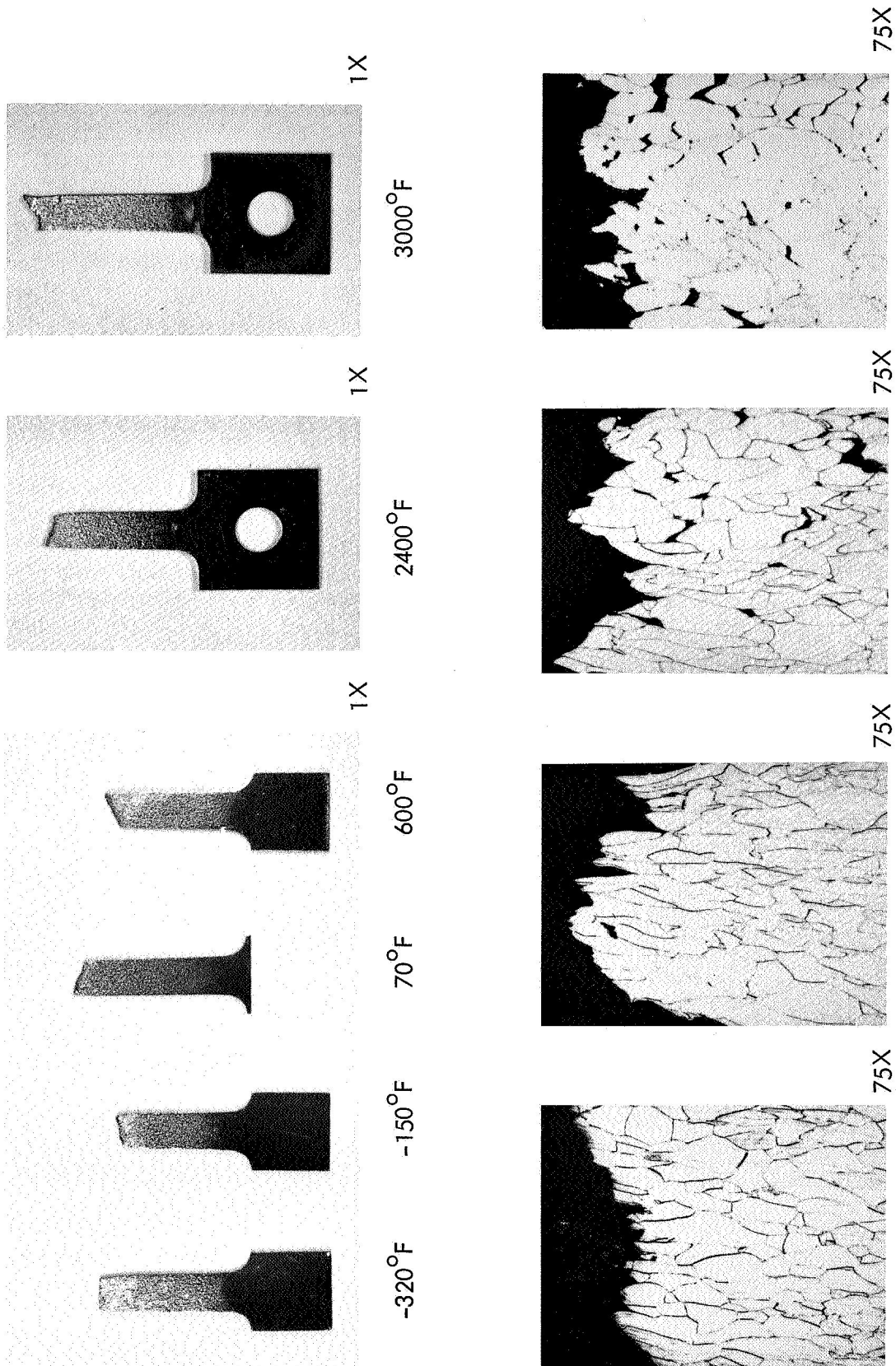


FIGURE 12 - Fracture Characteristics of ASTAR-811CN (Ta-7W-1Re-1Hf-0.012C-0.012N) as a Function of Test Temperature



Wedge-type grain boundary separations associated with relatively high stress-low temperature strain conditions were first observed in the ASTAR-811 specimen tested at 2200°F (1205°C) and in the ASTAR-811C and ASTAR-811CN specimens tested at 2400°F (1315°C), while round type grain boundary voids associated with lower stress-higher temperature strain conditions were first observed in the specimens tested at 200°F higher temperatures.

Mechanical twinning was observed in the ASTAR-811CN specimen tested at -320°F (-195°C). The mechanical twins, having serrated edges as shown in Figures 13a and 13b, are very similar in nature to those previously observed in the TIG welded ASTAR-811C tensile specimens also tested at -320°F (-195°C). Such twinning was only observed in precipitate free grains (i. e., none resolvable at 1500X), indicating that all of the carbon and nitrogen was either retained in solid solution or was present in the form of a submicroscopic, possibly coherent precipitate. Figure 13b suggests that some precipitation may be associated with the twinning process. Such precipitation could only occur from the interstitials retained in solid solution. The crystallographic nature of a number of the twins is well illustrated, especially in Figure 13b.

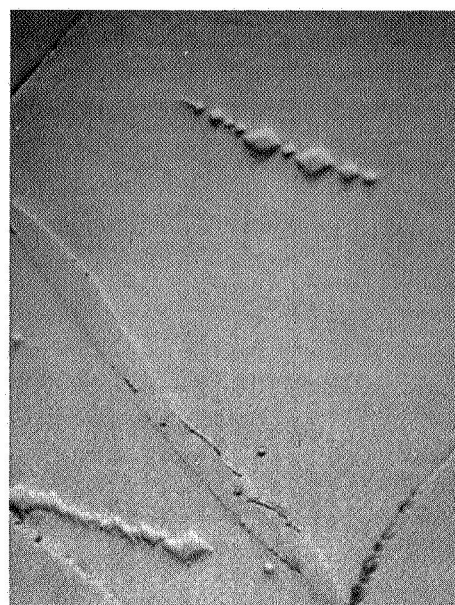
An unusual microstructure was also observed in the ASTAR-811CN specimen tested at 3000°F (1650°C). Near the fracture, extensive grain boundary migration was observed (Figure 13c), while indications of subgrain formation were present in local areas near grain boundaries. Precipitation of a fine, well dispersed matrix phase had also occurred during testing. Nearer the fracture surface, extensive subgrain formation was observed along the original grain boundaries (Figure 13d). Comparatively few grain boundary voids occurred in these areas compared to the adjacent areas not exhibiting similar microstructures (see Figure 12).

Longitudinal and transverse TIG welded tensile specimens were prepared and the tensile properties of these specimens are presently being determined as a function of temperature.



(a)

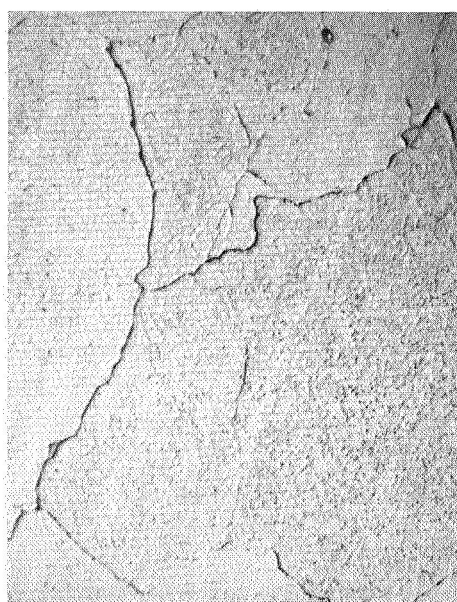
1500X



(b)

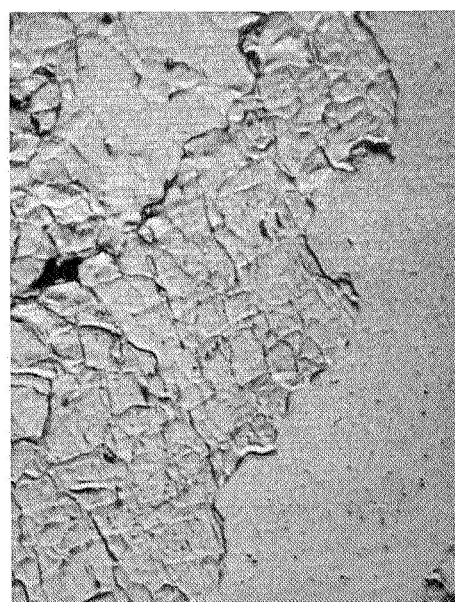
1500X

Tensile Specimen Tested at  $-320^{\circ}\text{F}$  ( $-195^{\circ}\text{C}$ )



(c)

500X



(d)

1500X

Tensile Specimen Tested at  $3000^{\circ}\text{F}$  ( $1650^{\circ}\text{C}$ )

**FIGURE 13 - Unique Microstructures of Two ASTAR-811CN  
(Ta-7W-1Re-1Hf-0.012C-0.012N) Tensile Specimens  
Oblique Light**

b. Creep — The creep properties of heats NASV-22 and NASV-23 (ASTAR-811 and ASTAR-811CN) will be determined over the temperature range of 2200–2800°F, on material annealed 1 hour at 3000°F prior to test. The data obtained this period is listed below in Table 7.

TABLE 7 - Creep Results<sup>(a)</sup> for ASTAR-811 (NASV-22) and ASTAR-811CN (NASV-23) at  $1 \times 10^{-8}$  Torr

Specimen	Test Temperature (°F)	Stress	Test Duration (hrs.)	Total Elongation (%)	Time to 1% Strain (hrs.)
NASV-22-1C	2200	19,000	826	6.4	185
NASV-23-1C	2600	8,000	382	5.4	172

(a) Material annealed 1 hour at 3000°F prior to test.

This data is plotted on Figure 14 normalized with the Larson-Miller parameter using 15 for the value of the constant. Also included on Figure 14 is data for ASTAR-811C (Heat NASV-20) and for T-111. The T-111 data are from tests conducted during the course of this investigation and also from the program being conducted at TRW<sup>(3)</sup>. Thus these data represent approximately 3–4 different heats of T-111 tested under ultra high vacuum conditions and annealed for 1 hour at 3000°F prior to test.

As is evident from the Larson-Miller normalization, quite a bit of data scatter exists between both sets of T-111 data. The data from Reference 3 were obtained primarily at 1800–2200°F while during their investigation, testing has been concentrated in the 2400–2600°F temperature range. The large body of experimental creep data indicate that the creep rate is given by the general equation<sup>(4)</sup>

$$\dot{\epsilon} = \sum_i A_i (\sigma, T, S) e^{-\Delta H_i (\sigma, T, S) / RT}$$

where  $A_i$  is the frequency factor and  $\Delta H_i$  the activation energy of one of a number of deformation

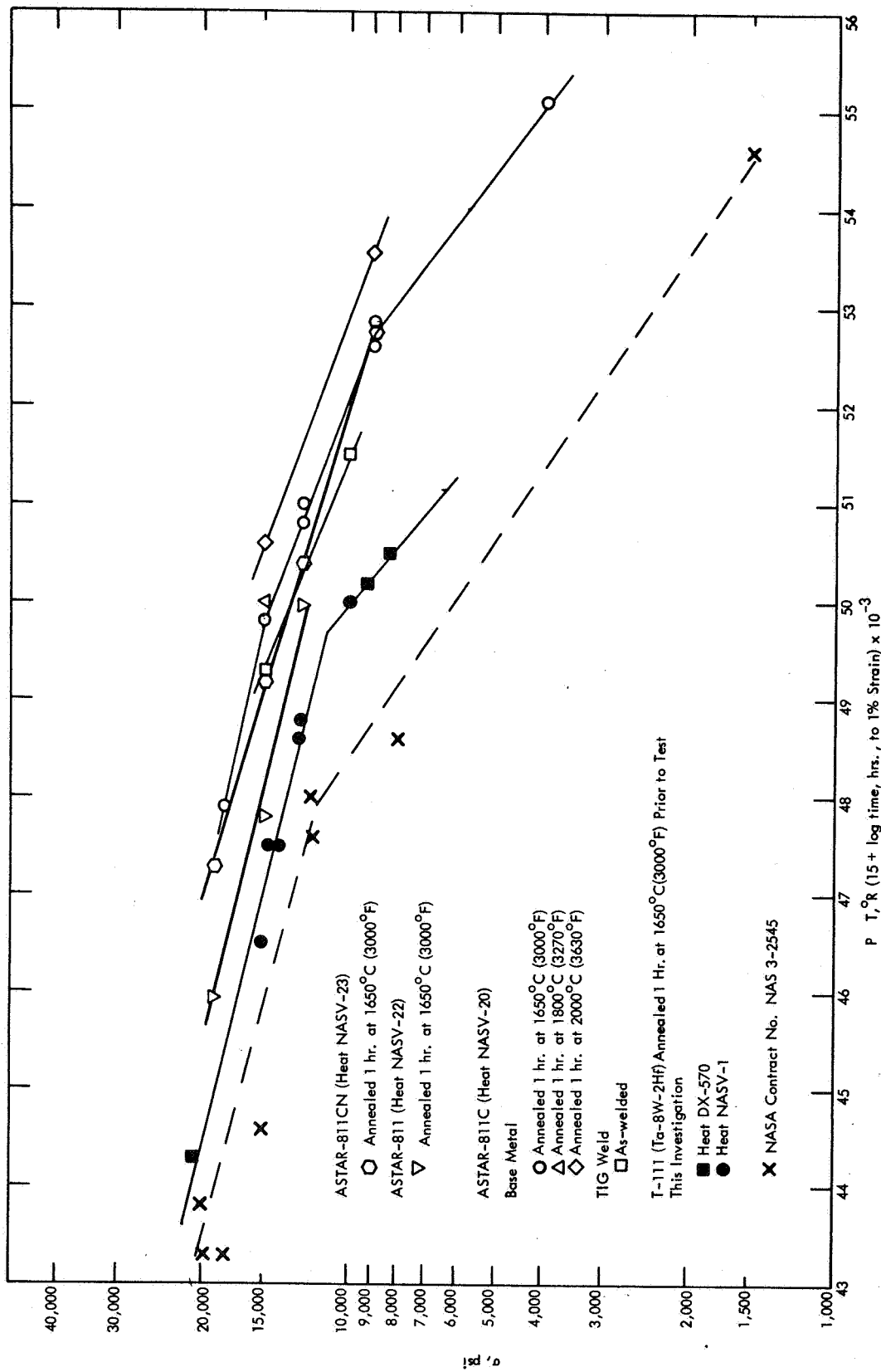


**FIGURE 14 - Creep Properties of ASTAR Tantalum Alloys**

mechanisms. Both  $A_i$  and  $\Delta H_i$  may depend on the stress ( $\sigma$ ) temperature ( $T$ ), and structure ( $S$ ). Thus to obtain the detailed creep equation, the constants  $A$  and  $\Delta H$  must be evaluated. However, the structure factor ( $S$ ) is particularly difficult to evaluate for it is not only affected by prior strain, stress, and temperature history but by their instantaneous value.

It has been shown by numerous investigators<sup>(5,6,7,8)</sup> that the experimentally determined secondary creep rate can be related to the applied stress under conditions of constant temperature and stress. Generally, it has been found that at low stress levels<sup>(5,6,7)</sup> the dependence of the secondary creep rate  $\dot{\epsilon}_S$  is given by:

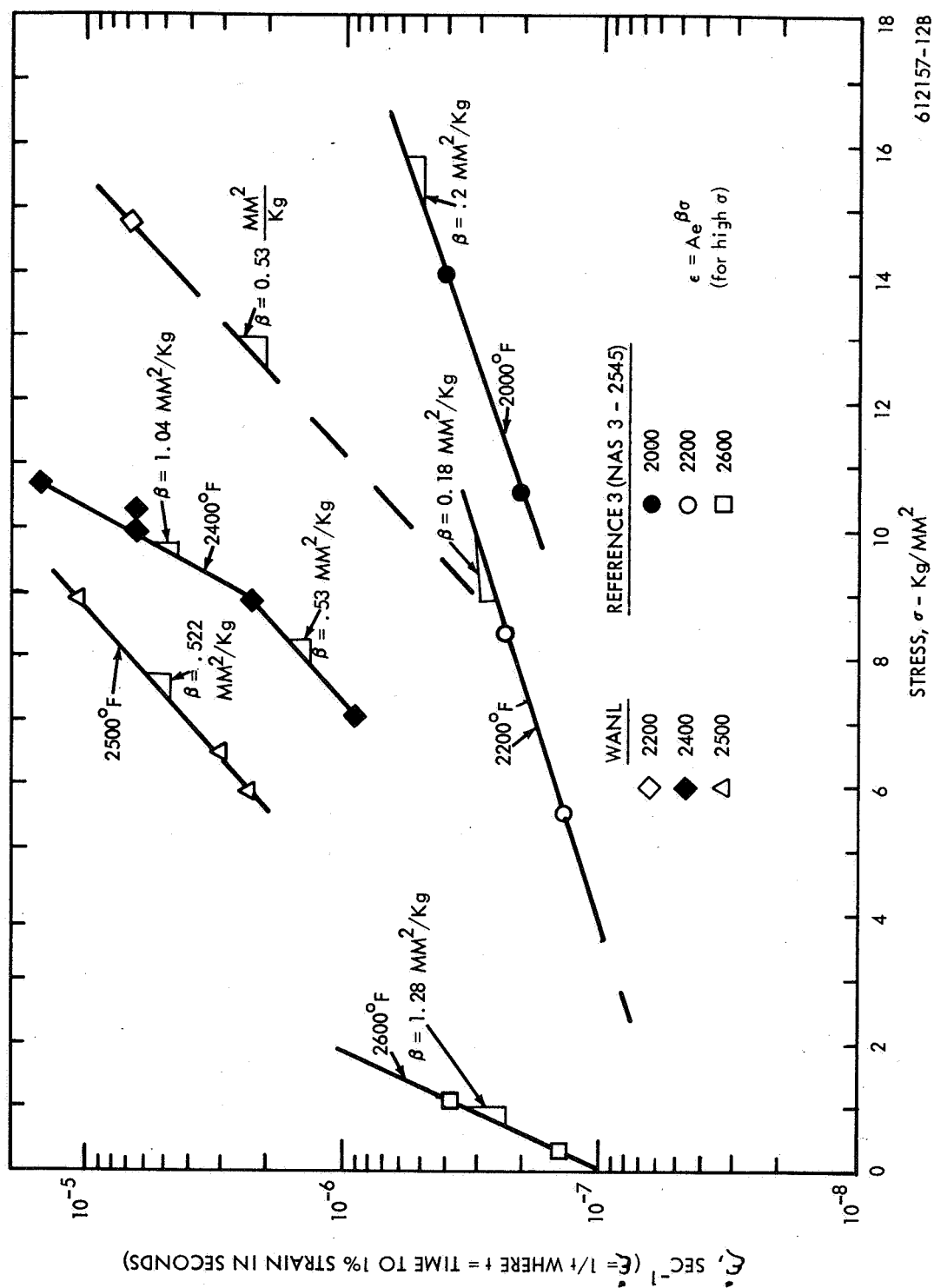
$$1. \quad \dot{\epsilon}_S = A\sigma^n$$

At high stress levels, the experimental results fit the relation:

$$2. \quad \dot{\epsilon}_S = A'e^{\beta\sigma}$$

For a constant temperature,  $A, A', n$  and  $\beta$  are constant. A model based on climb of edge dislocations from a pile-up array leads to a relation similar to that found experimentally at low stresses<sup>(7)</sup>. The T-111 creep data is plotted in Figures 15 and 16 using relations (1) and (2).

Since the shape of T-111 creep curves make it difficult to determine a minimum creep rate ( $\dot{\epsilon}_S$ ), the reciprocal of time to 1% creep ( $\frac{1}{t} = \dot{\epsilon}$ ) was substituted for  $\dot{\epsilon}_S$  and was the value used in plotting the data in Figures 15 and 16. It is evident from the data plotted in these two figures that the creep of T-111 is strongly a function of stress and temperature. Creep of the tantalum base alloys has been shown to be strongly structure sensitive<sup>(1,2)</sup> and T-111 behaves similarly. Thus it is not unexpected to see the rather poor fit of the T-111 creep data with the Larson-Miller parameter. It should be recognized that the Larson-Miller parameter is one of a number of time-temperature compensated expressions that have been proposed for the purpose of extrapolating creep-rupture results. These parameters are generally based on curve fitting procedures and were not derived from basic fundamentals of creep or creep rupture. Although creep rupture data for specific alloys within specified test conditions



612157-12B

FIGURE 15 - Creep Behavior of T-111

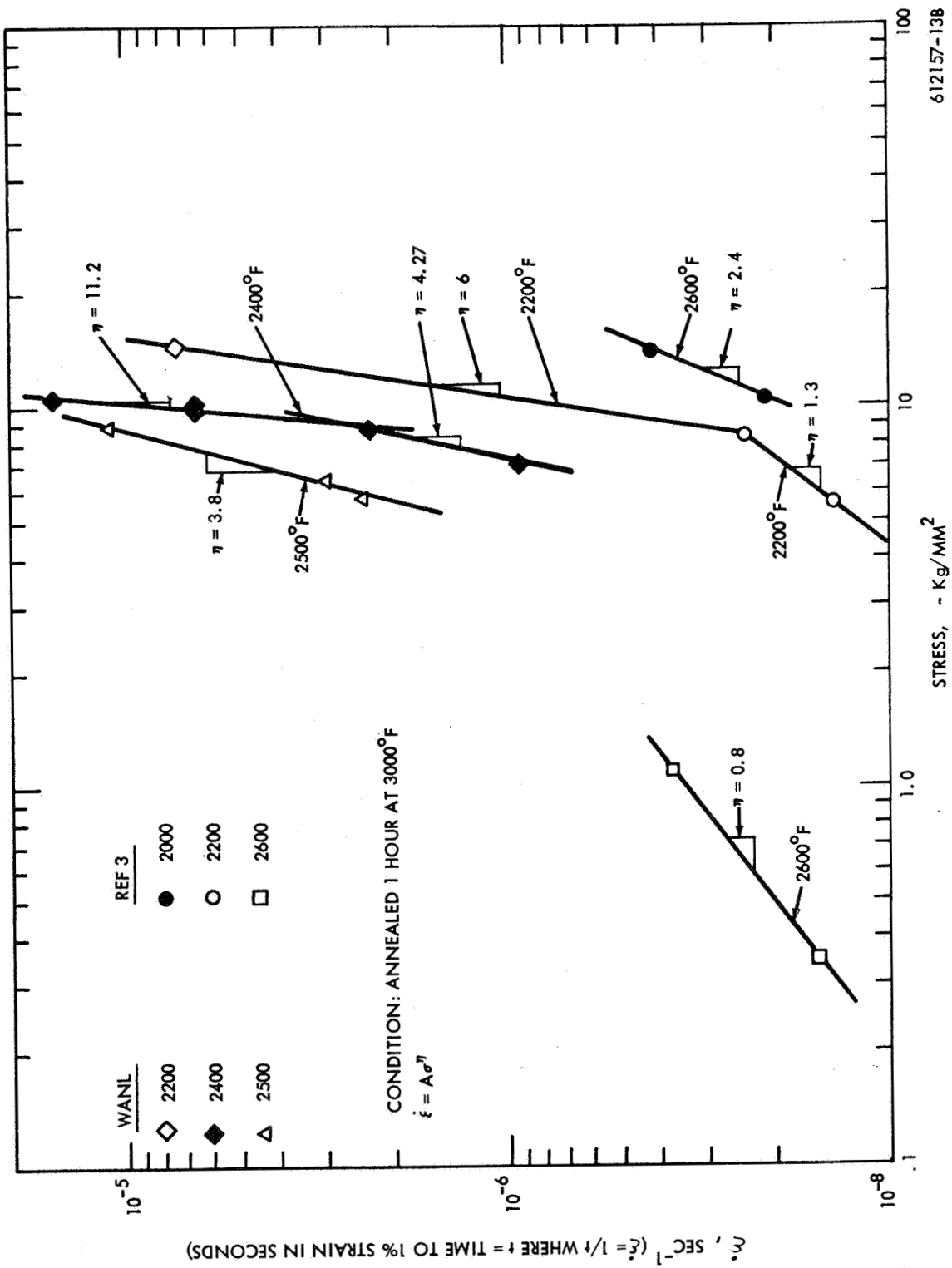


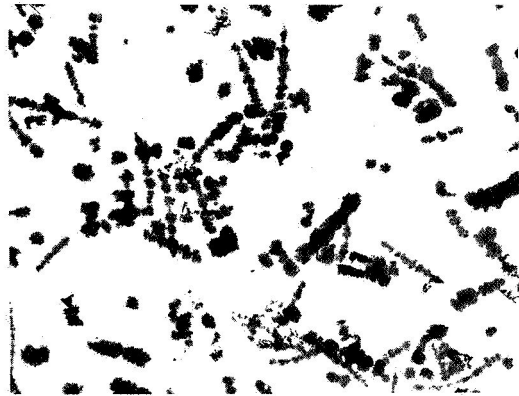
FIGURE 16 - Creep Behavior of T-111

have been described very well by these parameters, it would be fortuitous if they could be applied universally.

Since there are few reliable long time creep data points available for T-111, a thorough analysis of the creep behavior is not possible at this time. This is an area of investigation where much work remains to be done. The effect of heat treatment on the creep of ASTAR-811C<sup>(2)</sup> again illustrates the potent effect of the structure factor.

Phase Identification and Morphology — The dispersed phases present in as-cast ASTAR-811 and ASTAR-811CN were extracted in the standard 10 ml bromine-90 ml methanol-10 grams tartaric acid solution. X-ray diffraction analysis of the ASTAR-811 residue indicated that only residual BCC tantalum matrix was present. The lack of a second phase in this alloy is consistent with its clean microstructure, as shown in Figure 6. Residual BCC tantalum matrix and a lesser amount of the HCP tantalum dimetal carbide phase were present in the ASTAR-811CN extraction. This extraction was then examined by transmission electron microscopy and selected area electron diffraction. The size and shape of the HCP phase are shown in Figure 17 along with typical diffraction patterns. The precipitate is in the form of thin platelets, approximately 0.3 to 1 $\mu$  in diameter (Figures 17a and 17b), and in the form of thin elongated platelets. This latter form of precipitate appears to be comprised of a number of the smaller platelets which apparently nucleated along low angle subgrain boundaries and grew together to form the elongated platelets (Figures 17a and 17c). These results are in good agreement with the microstructure of ASTAR-811CN as illustrated in the eleventh quarterly progress report<sup>(2)</sup>. An internal structure is apparent in all of the platelets as illustrated in Figures 17b and 17c. This internal structure is apparently caused by faulting and/or microtwinning as illustrated by the streaks in the electron diffraction ring pattern shown in Figure 17e. The sharp, continuous rings are those of aluminum, which was used for calibration purposes.



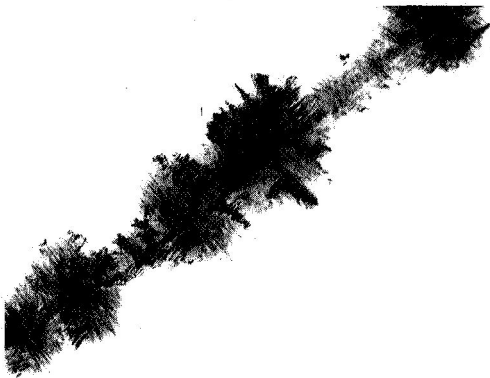


3,000X

(b)

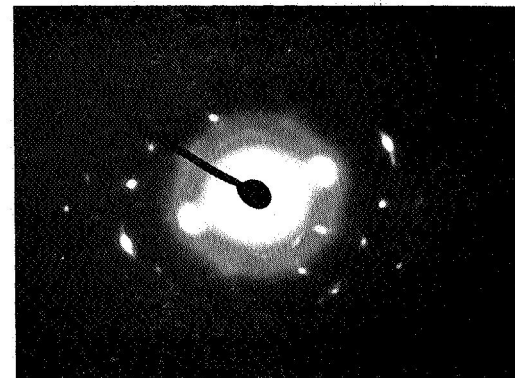


25,000X



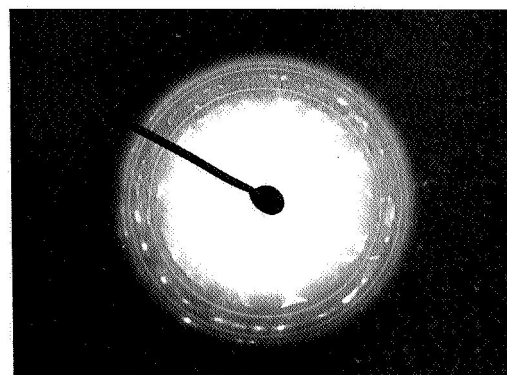
(c)

30,000X



(d)

SAED of c



(e)

DP

FIGURE 17 - Transmission Electron Micrographs of HCP Tantalum Dimetal Carbide Precipitate Extracted from As-Cast ASTAR-811CN (Ta-7W-1Re-1Hf-0.012C-0.012N)

Other studies are presently being conducted on ASTAR-811CN sheet to determine the phase relationships present in this carbon and nitrogen containing alloy as functions of temperature and time at temperature.

### III. FUTURE WORK

During the next period, the following will be accomplished.

1. Complete evaluation of the mechanical properties of ASTAR-811 and ASTAR-811CN.
2. Initiate study on the effect of post weld thermal treatment on the ductile-brittle transition temperature of ASTAR-811CN.
3. Continue phase identification and morphology investigation.

#### IV. REFERENCES

1. R. W. Buckman, Jr. and R. T. Begley, "Development of Dispersion Strengthened Tantalum Base Alloy", Final Technical Report, Phase I, WANL-PR-(Q)-004.
2. R. W. Buckman, Jr. and R. C. Goodspeed, "Development of Dispersion Strengthened Tantalum Base Alloy", 11th Quarterly Progress Report, WANL-PR-(Q)-012.
3. J. C. Sawyer and E. A. Steigerwald, "Generation of Long Time Creep Data of Refractory Alloys at Elevated Temperatures," 13th Quarterly Report on Contract NAS 3-2545.
4. H. Conrad, "Experimental Evaluation of Creep and Stress Rupture", Mechanical Behavior of Materials at Elevated Temperature, Edited by J. E. Dorn, McGraw-Hill, 1961.
5. J. E. Dorn, Creep and Recovery, p 255, ASM, Cleveland, Ohio.
6. J. J. Kanter, AIME Trans. 1938, Vol. 131, p 385.
7. J. Weertman, J. Appl. Physics, 1955, Vol. 26, No. 10, p 1213.
8. P. Feltham and J. D. Meakin, Acta Met, 1959, Vol. 7, p 614.